GEORGIA INSTITUTE OF TECHNOLOGY — OFFICE OF CONTRACT ADMINISTRATION

PROJECT ADMINISTRATION DATA SHEET

[X] ORIGINAL [ ] REVISION NO. _____

Project No. E-18-617 (R6098-0A0) GTRC/~~GKK~~ DATE 3 / 3 / 86

Project Director: S. R. Stock School/~~Dept~~ Materials Engineering

Sponsor: National Science Foundation

Type Agreement: Grant No. INT-8513629

Award Period: From 3/1/86 To 8/31/88 (Performance) 11/30/88 (Reports)

Sponsor Amount:	This Change	Total to Date
Estimated:	$	$ 9,350
Funded:	$	$ 9,350

Cost Sharing Amount: $ 95. Cost Sharing No: N/A

Title: Synchrotron Radiation Studies of the Spatial Distribution of Impurities in Materials

ADMINISTRATIVE DATA — OCA Contact John B. Schonk x-4820

1) Sponsor Technical Contact:

Christine Glenday
National Science Foundation
STAI/INT
Washington, D. C.
Phone: 202/357-7554

2) Sponsor Admin/Contractual Matters:

Dionie Henry
National Science Foundation
DGC/STIA
Washington, D. C. 20550
Phone: 202/357-9602

Defense Priority Rating: N/A Military Security Classification: N/A

(or) Company/Industrial Proprietary: N/A

RESTRICTIONS

See Attached NSF Supplemental Information Sheet for Additional Requirements.

Travel: Foreign travel must have prior approval – Contact OCA in each case. Domestic travel requires sponsor approval where total will exceed greater of $500 or 125% of approved proposal budget category.

Equipment: Title vests with GIT

COMMENTS:

No funds may be expended after 8/31/88, even though 90 days are allowed for report presentation.

* Includes a six month unfunded flexibility period.

COPIES TO: SPONSOR'S I. D. NO. 02.107.000.85.111

Project Director
Research Administrative Network
Research Property Management
Procurement/GTRI Supply Services
Research Security Services
Reports Coordinator (OCA)
GTRC
Library
Project File
Other Jones/ Legal

2

NV-SR1,714-2

GEORGIA INSTITUTE OF TECHNOLOGY
OFFICE OF CONTRACT ADMINISTRATION

NOTICE OF PROJECT CLOSEOUT

Date 3/31/89

Project No. E-18-617 Center No. R6098-0A0

Project Director S. R. Stock School/Mat. Mat. Eng.

Sponsor National Science Foundation

Contract/Grant No. Grant No. INT-8513629 GTRC X GIT ___

Prime Contract No. ___

Title Synchrotron Radiation Studies of Spatial Distribution of Impurities in Material

Effective Completion Date 11/30/88 (Performance) 2/28/89 (Reports)

Closeout Actions Required:

X None
___ Final Invoice or Copy of Last Invoice
___ Final Report of Inventions and/or Subcontracts
___ Government Property Inventory & Related Certificate
___ Classified Material Certificate
___ Release and Assignment
___ Other ___

Includes Subproject No(s). ___

Subproject Under Main Project No. ___

Continues Project No. ___ Continued by Project No. ___

Distribution:

X Project Director
X Administrative Network
X Accounting
X Procurement/GTRI Supply Services
X Research Property Management
___ Research Security Services
X Reports Coordinator (OCA)
X GTRC
X Project File
X Contract Support Division (OCA)
___ Other ___

GEORGIA TECH 1885-1985

DESIGNING TOMORROW TODAY

Georgia Institute of Technology
School of Materials Engineering
Atlanta, Georgia 30332-0245
(404) 894-6882

May 22, 1987

Ms. Christine Glenday
National Science Foundation
International Programs
US-UK Cooperative Science Program
Washington, D. C. 20550

Dear Ms. Glenday:

Accompanying please find my report for the research done to date under Grant No. INT-8513629,"Synchrotron Radiation Studies of the Spatial Distrbution of Impurities in Materials." I am also enclosing two reprints which resulted from work supported by this grant.

I am looking forward to another fruitful year of cooperative research with my colleagues in Britain.

Sincerely yours,

Stuart R. Stock
Assistant Professor

Annual Report for

U.S.-U.K. Cooperative Science - Synchrotron Radiation Studies of the Spatial Distribution of Impurities in Materials

Grant No. INT-8513629

by

Stuart R. Stock
Assistant Professor

School of Materials Engineering
Georgia Institute of Technology

Submitted to:

Ms. Christine Glenda y

National Science Foundation
U.S.-United Kingdom Cooperative Science Program
Washington, D.C. 20550

Abstract

Two collaborative experiments, one on synchrotron computed tomography (SCT) and one on topographic EXAFS, have been conducted in the first year of this U.S.-U.K. Cooperative Science program. One paper on the SCT experiments has been published, and this work led directly to a funded project (ENG/MSM, NSF) supporting SCT experimentation at the National Synchrotron Light Source (NSLS) and to a significant portion of an NSF-MRG proposal which is currently under review. During the second year of the program, experiments using synchrotron x-ray microbeam fluorescence analysis and mapping of trace elements will be conducted, and the SCT experiments will continue on either Si_3N_4 + SiC composites or crept, polycrystalline Cu-Sb specimens. A proposal for continuation of this cooperative program is planned.

Table of Contents

I. Report of Progress

Research during the first year focused on radiographic measurements and on topographic EXAFS experimentation. In the past two years, very high resolution synchrotron computed tomography (SCT) has developed rapidly, and SCT offers considerable advantages over conventional projection radiography. This, coupled with the fact that the British collaborating scientists are leading the development of SCT, dictated a shift in effort from differential absorption radiography to the analogous SCT techniques. A proposal for beam time at Daresbury was approved, and a short series of scans of a porous alumina refractory were performed during May 1986 at Daresbury.

Daresbury was unavailable from October 1986 to June 1987 due to the installation of the new high brightness lattice. To keep the momentum developed earlier, D.K. Bowen's and the author's groups conducted collaborative topographic EXAFS experiments in April 1987 at the Stanford Synchrotron Research Laboratory (SSRL). A non-stoichiometric GaAs crystal and a hematite crystal were examined.

Despite the shutdown of Daresbury, two of the three proposed methods have been examined in the first year of the two-year program: x-ray absorption and topographic EXAFS. The experimental program for the topographic EXAFS is complete and that for x-ray absorption is continuing. Two of the five specimen types have been examined: porous sintered specimens and specimens for topographic EXAFS. The accomplishments during the

first year and the first two research trips meet our expectations for successful completion of the program. Through careful planning, our expenditures have been less than anticipated, and additional research trips will be possible under the present budget. The paragraphs below describe the specific work accomplished thus far in the program.

I.1 Synchrotron Computed Tomography (SCT)

The SCT of alumina was conducted at the Daresbury Topographic Wiggler Station under the author's exploratory grant (for beam time) "Synchrotron Computed Tomography Study of the Distribution of Pores in Sintered Alumina." The apparatus used is diagrammed in Fig. 1 and was designed and constructed by Dr. J.C. Elliott, London Hospital Medical College and by Dr. D.K. Bowen, University of Warwick. Image reconstruction was done using software of Dr. S.D. Dover, King's College, London.*

The spatial profiles of absorption in a thin slice of material are recorded for a large number of projection directions in CT. At this level CT involves the same principles as conventional radiography. In CT, however, the large number of absorption profiles are combined via a Fourier transformation to reconstruct uniquely the spatial position and absorbing power of each volume element within the slice. A three-dimensional representation of the distribution of absorption is obtained by recording adjacent slices.

---

* For more information, see accompanying reprints.

Highest resolution requires either a wide, but parallel, x-ray beam and a detector with multiple micrometer-sized elements or a pinhole collimator and a normal detector. The latter approach is more practical and was used for our experiments. Therefore, the specimen was translated across the beam to build up each absorption profile. After each profile was obtained, the specimen was rotated by 3.0 degrees, and the process was repeated until the specimen had been viewed from 180 degrees.

The collimator diameter was 10μm and the translation steps were 15μm. The counting time was 0.75 seconds per position. Absorption was measured for x-rays with λ=0.37A by means of a post-specimen monochromator. Figure 2 shows absorption profiles (intensity vs. position) for seven projection directions (18 degrees difference for first and last scans) through the alumina sample. The transmitted intensity profile for each succeeding projection direction is offset along the unlabeled axis. The flat portions of the curves represent positions at which the beam is not intersecting the specimen.

In the limited beam time, five slices of the 2x2x10 mm alumina sample were obtained. Four of the five scans were made with a 10μm diameter collimator and are from adjacent volumes of material (each slice is separated by 20μm). The other scan was recorded using a 30 μm diameter collimator. A typical reconstructed slice is shown in Fig. 3. The grey scale represents absorption, with decreased absorption shown by darker shades. A number of pores and a crack or very large cavity

intersecting the surface are seen.

The results from this experiment were included in a paper in SPIE Vol. 691 X-ray Imaging II. The experience gained with SCT led to the NSF program "High Resolution Synchrotron Computed Tomography for Engineering Applications" (grant no. MSM-8614493, $29,986, 2/15/87 - 7/31/88). We have also proposed, based on our Daresbury experience, a more substantial program as part of an NSF-MRG proposal entitled, "Structure, Deformation, and Fracture Mode Characterization of Anisotropic Materials." Both the project and proposal are aimed at developing synchrotron capabilities similar to those at Daresbury.

I.2 Topographic EXAFS

The topographic EXAFS experiments on GaAs and on hematite crystals were only recently completed, and no analyses of the results are presently available. The experiments were conducted at SSRL because of the Daresbury shutdown and Dr. Bowen's sabbatical in the U.S. The two specimens examined (on SSRL Beam Line II-4) were expected to have significant spatial variation in stoichiometry or in valence state, and the goal of the experiments was to investigate the sensitivity of topographic EXAFS to this spatial variation.

A particular reflection for each sample was chosen to minimize the harmonics contained in the topographic image (e.g. h=220 for GaAs) and to enhance any topographic EXAFS contrast. The specimen was aligned normal to the beam and then rotated so

that the reflection of interest was diffracted in transmission and at a wavelength near that of the absorption edge (Ga for GaAs and Fe for Fe_2O_3). Further alignment was accomplished by recording in situ transmission Laue patterns: with an incident white beam many diffraction spots are formed, each with a different wavelength.

We attempted to monitor the critical reflection using a Brimrose x-ray videocamera system, but the background was too high for the fine structure to be resolved within the spot. We located the edges of both the GaAs and Fe_2O_3 crystals by exposing a large number of polaroids and observing whether the contrast changed after small rotations. Topographs were recorded at wavelengths on either side of the absorption edges using the minimum rotation steps of the SSRL topography camera. The change in contrast is so gradual that detailed numerical image analysis will be required before this experiment can be evaluated. The image analysis will be conducted by the British group using Daresbury Laboratory facilities.

II. Problems and Favorable Developments

The SCT characterization of the alumina sample looks very promising. This activity will be expanded in the second year of the program. The nine month shutdown of Daresbury and the accompanying logjam of experiments could have posed great difficulty, but we were able to obtain time at SSRL during which we could continue the collaborative research. The poor

performance of the Brimrose videosystem (which, to be fair, may have been malfunctioning) seriously hindered our topographic EXAFS research.

The final problem we wish to report is embarrassing. Our collaborators wrote the enclosed paper of the SCT experiments, and a clerical error excluded proper acknowledgment to NSF for the author's participation in these experiments. This was compounded by the fact that the manuscript was sent to the author's former address where it was not forwarded for several months. By the time he saw the omission, the paper had already been published. The author deeply regrets this failure.

III. Program During 1987-88

During the last year of the program, microbeam fluorescence analysis and mapping experiments will commence and SCT characterization will continue. Microbeam experiments at Daresbury are scheduled by the British group for next Fall, and the author will participate in these runs. A proposal for more SCT beam time, also at Daresbury, is currently being prepared; the earliest this could be scheduled is next Winter.

The role of the author in the microbeam fluorescence experiments will primarily be that of an assistant: this is the best means of gaining the experience required to establish a similar program at Georgia Tech. We hope to examine the spatial variation of impurities in two types of specimens of especial interest to us. The first is In doped GaAs crystals and the

second is specimens with grain boundary segregation. We have one GaAs crystal where the striations from In segregation are visible in x-ray topographs and are separated by 100μm distances. No precise measurements have yet been reported on the spatial variation of In concentration. Techniques such as SIMS confirm that there is a variation but cannot conclude much else; the impact of successful x-ray fluorescence microprobe experiments will be substantial. Two different material systems are being considered for the attempt to measure segregation at grain boundaries: Cu-Sb and Cu-Bi. A study of either system would have considerable impact on our understanding of grain boundary embrittlement, and we will attempt to detect Sb or Bi at the Cu grain boundaries.

Two sets of specimens are currently being prepared for SCT examination. The first material is Cu-Sb, and the second is Si_3N_4/SiC composite. We would like to examine both sets of specimens, but beam time constraints may force a choice between the two.

The Cu-Sb samples are polycrystalline and have been heat treated to produce heavy Sb segregation to the grain boundaries. Grain boundary cavities form in response to loading at 400^{o}C. We are currently investigating the relationship between crack tip damage and fracture mechanics concepts such as C_t and C^* (the time dependant analogs of the J-integral) under the direction of Professor A. Saxena, School of Materials Engineering, Georgia Tech. While it is fairly simple to observe the cavity size and

spatial distributions on fracture surfaces, it is impractical to characterize these distributions away from the fracture surface. We will machine cylindrical specimens from various positions in the specimen and will examine slices from the middle as well as near the surface of the compact tension specimens. There could be significant differences between near-surface and interior regions and at different distances from the crack tip. Conventional synchrotron radiography will be used to supplement the SCT measurements.

The Si_3N_4/SiC composites have been reaction sintered. In the SCT experiments we will attempt to differentiate between the following: completely reacted Si_3N_4, pores in the Si_3N_4, unreacted Si due to poor firing and SiC fibers. Differences in firing may cause some of the defects, and considerable porosity can be retained if the green composite is not de-aired prior to firing. Pores as large as 300μm diameter have been observed by Dr. T. Starr (Georgia Tech Research Institute) who is providing these samples. A number of slices will be examined from combinations of good/poor firing and de-airing/no de-airing. These measurements may also be supplemented by conventional synchrotron radiography.

If these experiments are successfully completed, we will have examined all of the techniques and all of the specimen types listed in the proposal, excepting perhaps the precipitates in coal. The Si_3N_4/SiC composite, however, is a severer test of SCT's ability to detect precipitates and to differentiate between

porosity and precipitates, and we will use it instead of coal.

In the coming months we will submit a proposal for continued research using synchrotron x-ray methods such as SCT and microbeam fluorescence mapping.

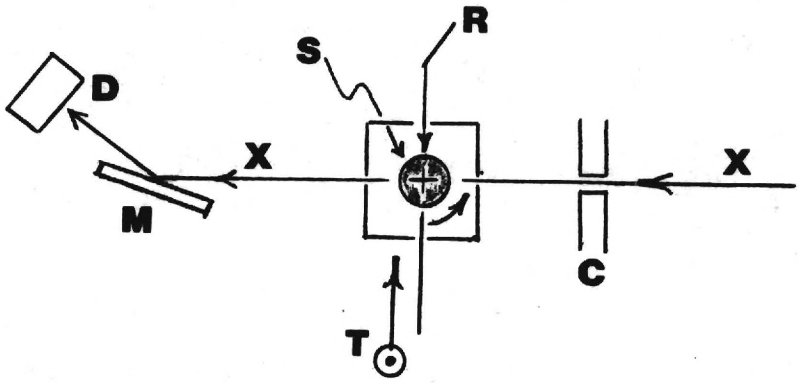

Figure 1. Schematic diagram of the Synchrotron Computed Tomography (SCT) apparatus. X, X-ray beam; C, collimator; T, translation axes; R, rotation axes; S, sample; M, monochromator and D, detector.

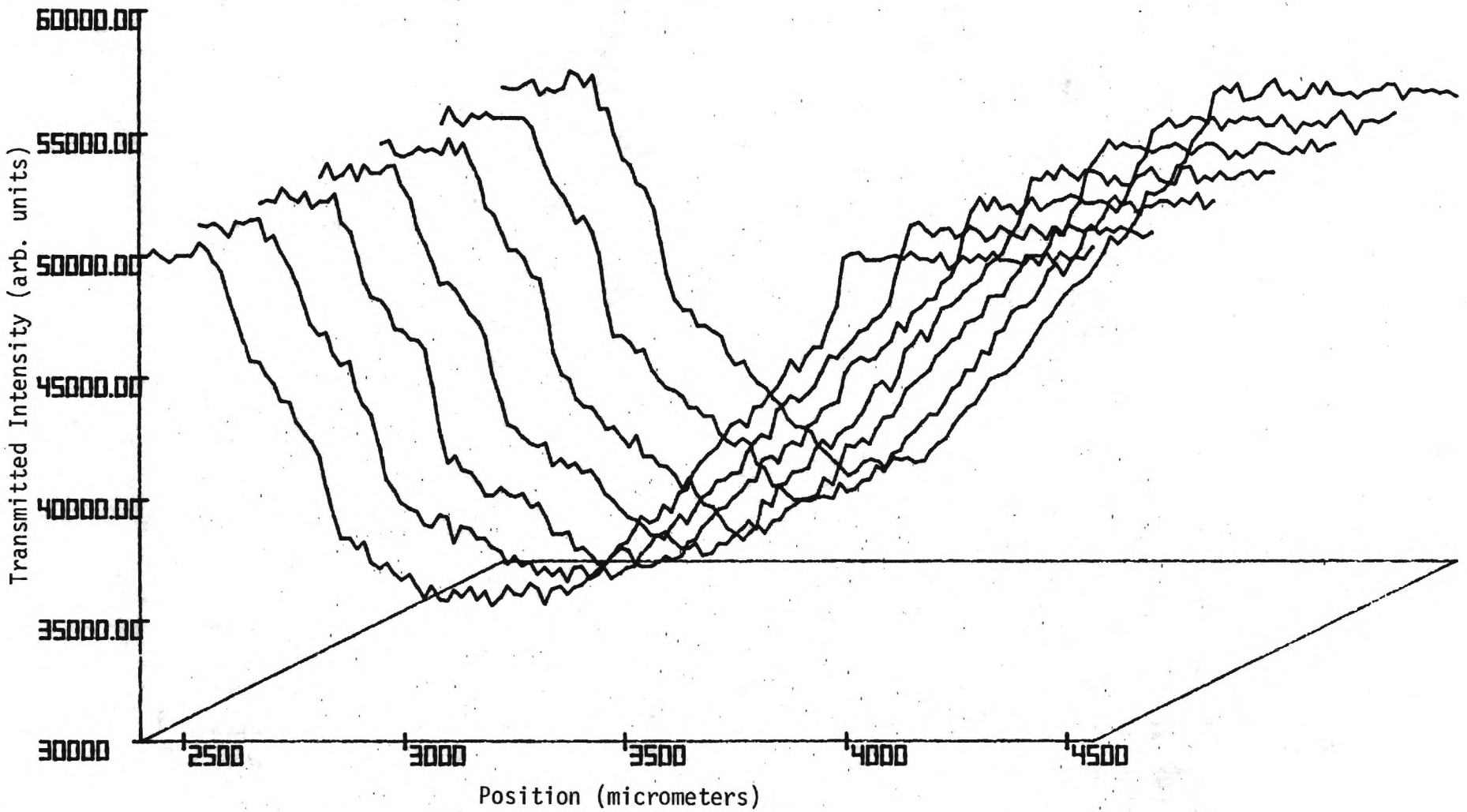

Figure 2. Transmitted intensity as a function of position for an alumina specimen. Profiles are shown for seven projection directions. The successive profiles were produced by three degree rotations and are indicated by the displacement along the unlabeled axis.

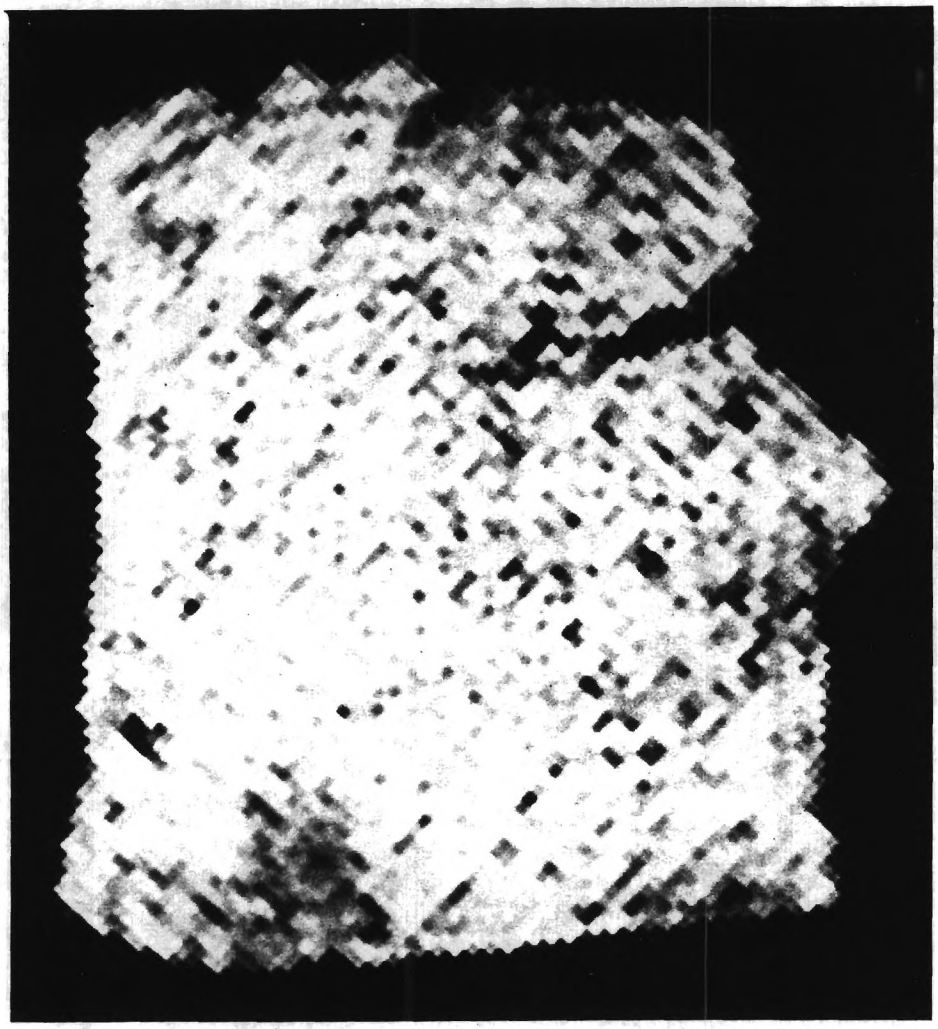

Figure 3. Synchrotron computed tomograph of alumina. The sides of the slice are 2mm, and the darker pixels represent decreased x-ray absorption. This tomograph was produced with a 10 micrometer diameter collimator and 0.37 A radiation.

Appendix

X-ray Microtomography with synchrotron radiation

D.K. Bowen[1]

Department of Engineering, University of Warwick, Coventry CV4 7AL, U.K.

J.S. Elliott[2]

Department of Biochemistry, London Hospital Medical College, London, U.K.

S.R. Stock[3]

Department of Materials Engineering, Georgia Institute of Technology, U.S.A.

S.D. Dover[4]

Department of Biophysics, King's College, London, U.K.

Abstract

High resolution x-ray microtomography has been established at the synchrotron radiation source at Daresbury Laboratory, U.K. A high precision mechanical stage with two translational and one rotational degree of freedom has been constructed, and fully characterised by mechanical metrology; overall precision is better than 0.5 μm. Collimation of the incident synchrotron radiation beam through a 4 μm aperture has been obtained, giving 2 μm overall spatial resolution. Results have been obtained using monochromatic radiation at both 1 angstrom and 0.37 angstrom wavelengths, on human bone fragments and on sintered alumina ceramics.

Introduction

Since the invention of computerised axial tomography by Hounsfield in 1973[1] it has attracted enormous development in the medical imaging field. This development has concentrated primarily upon the reduction of the data collection time and x-ray dose, for obvious medical reasons, by the use of multiple sources and detectors and by the design of efficient algorithms for reconstructing the images. Relatively little attention has been paid to the accurate quantification of the absorption parameters derived nor to the ultimate spatial resolution that can be attained. This is primarily due to technological limitations, in that conventional x-ray sources are not very bright, nor can intensity be sacrificed in order to produce monochromatic radiation although the latter is necessary for quantitative measurements since the absorption parameters vary rapidly with wavelength.

In part due to the advent of very bright synchrotron radiation sources, there has recently been a surge of interest in the application of computerised axial tomography, with high spatial resolution and accurate quantification of absorption parameters, to the field of non-destructive testing of biological and mechanical materials; see for example Reimers, Gilboy and Goebbels[2]. Tomographs with resolution around 10 μm have been obtained, though with data collection of one or two days, on laboratory microfocus x-ray sources by Elliott and Dover[3,4] and have been most encouraging in demonstrating the potentiality of the method for non-destructive imaging. It is especially useful for materials that are delicate or friable, or in which important microstructural features can be lost during specimen preparation. For example, in bone or loosely sintered ceramic composites the measurement and visualisation of porosity is an important requirement, yet pores may be artificially enlarged by additional fragments breaking off during specimen preparation or by any etchants that are necessary to remove polishing damage. In soft plastic materials, whether metal or polymers, the precise morphology of voids and second phases may be grossly distorted by smearing or other distortions during sectioning and polishing for conventional metallography. In addition, the physical sectioning methods are of course totally destructive, and are usually the last measurements that can be made upon those specimens. There is therefore very considerable interest in the application of the non-destructive computerised axial tomographic methods to the imaging of density changes (pores or voids, second phases, fibre or particle inclusions etc.) in both biological and non-biological materials. For the highest resolution, the brightness requirements virtually dictate the use of a synchrotron radiation source though with efficient parallel detection assemblies conventional x-ray sources or radioactive gamma ray sources have powerful applications.[2]

This paper describes the application of the synchrotron radiation source at Daresbury Laboratory to the production of high resolution tomographs of both bone fragments and of sintered alumina specimens.

Instrumentation

The system has been used on two different beam lines at Daresbury Laboratory, from a conventional bending magnet and from the high field superconducting "wiggler" magnet, respectively. The former gives excellent intensity in the one to two Angstrom wavelength regime, and the latter, in the 0.2 - 1.5 Anstrom regime although in each case the total useable spectrum is much wider. In both cases the "double crystal camera" described by Bowen and Davies[2] was used for mounting and alignment of the microtomography stage, collimators, monochromators and detectors. The standard Daresbury Laboratory control software, written by E. Pantos, was used to control all the translations and rotations of the stage and monochromator and to collect the data from the detectors. The incident beam was collimated by a platinum aperture, centered on a steel cylinder. A V-block was mounted on a small optical bench so that when the collimator assemblies were dropped on to the V they were accurately centered in the incident white radiation beam. Thus, exchange of collimators could be made very rapidly without upsetting the alignment. The specimen was placed within two or three millimetres of the collimating aperture, and with the long source to collimator length of 60 m (conventional magnet) or 40 m (wiggler magnet) the source was in all cases demagnified to less than 1 μm diameter at the specimen. In all cases the blurring due to both Fresnel and Fraunhofer diffraction is very much less than 1 μm with this arrangement. After passing through the specimen, the beam was diffracted by a graphite monochromator, which delivered a broad band (approximately 5%) monochromatised beam to the scintillation counter detector. This was run through a single channel analyser in order to minimise the effect of $\lambda/2$ harmonics. The incident beam was monitored with either an ion chamber before the collimator or with a scintillation counter measuring scattered radiation, in order to compensate for the gradual decay in synchrotron radiation intensity with time after the storage ring has been filled.

Considerable attention was paid to the design of the tomographic stage itself. The design is based upon kinematic and elastic design principles, and utilises accurately ground tungsten carbide balls of diameter 0.375 ± 0.000025". One of these was cemented at each end of a 15 cm spindle with epoxy resin, and another short spindle to carry the specimen at its tip or cemented on to one of the balls diametrically opposite the main spindle. Both balls rested in V-blocks whose bearing surfaces were formed by 5 mm diameter polished sapphire discs. These ball/V-block assemblies are the basic rotational and linear bearings. One V-block was fixed and had a horizontal micrometer head mounted coaxially with a specimen spindle so that the ball sitting in the V could rest against the micrometer spindle face. The other V-block was mounted on a beryllium-copper parallelogram spring and positioned over a vertical micrometer head whose curved spindle tip bore on a polished sapphire plate fixed on to the lower surface of the V. Rotation of this micrometer moves the specimen vertically and provides the basic high precision stepping motion across the narrow x-ray beam to measure each projection. The specimen spindle could be rotated by a spur gear mounted directly on it near the fixed V which meshed with another smaller gear displaced horizontally from it: this arrangement ensures a minimal change in the meshing of the gears as the specimen is moved in a vertical direction. This arrangement of mounting the spindle conforms with the kinematic principle that requires the minimum number of constraints but allows rotation and two translations. High precision micrometer heads and gears were used in the construction.

The performance of the stage under computer control was extensively studied in the Centre for Microengineering and Metrology, Warwick University. As previously reported[6] the performance of the stage was considerably better than the necessary 1 μm; the results are summarised in Table 1.

Table 1. Results of Metrology on Microtomography stage.

Axis 1 (translation)	
Backlash	< ± 0.1 μm
Accuracy over 90 μm	± 0.1 μm
Accuracy over 600 μm	± 0.3 μm
Settling time to 0.1 μm	100 ms
Axis 2 (rotation)	
Centre location precision over 360° rotation	± 0.1 μm
Axis 3 (translation)	
As for Axis 1	

A photograph of the stage is shown in Figure 1.

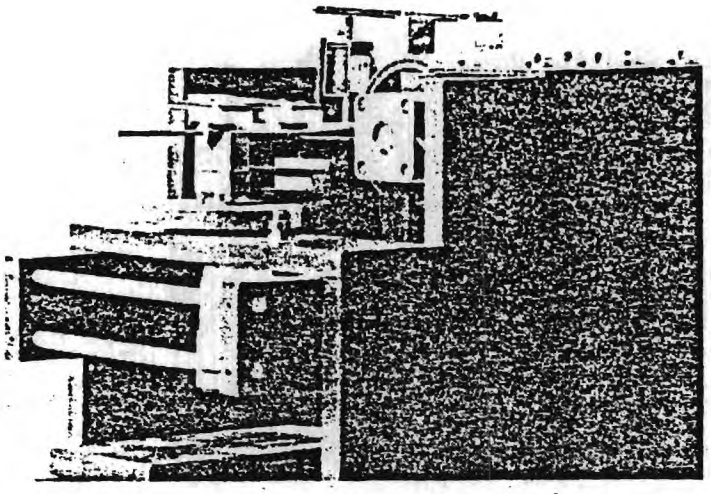

Figure 1. Photograph of the Microtomography stage.

Results and discussion

A typical data collection routine comprised sixty-four projections separated by angles of 3°, each of which consisted of 128 separate measurements during the vertical scan. The step distance between measurements in the vertical scan direction was chosen to match the collimator used; 5 μm for the 4 μm collimator and 15 μm for the 10 μm and also for the 30 μm collimator. By the Nyquist theorem, the spatial resolution that can be expected is one-half of the spatial sampling frequency. Thus, for the 4 μm aperture and 5 μm steps we expect 2/2.5 μm resolution.

Figure 3 shows a "section" of a piece of human femur bone taken at 2/2.5 μm resolution. The three prominent circular features are Haversian canals, and the shading indicates regions of reduced/increased mineralisation surrounding them. Figure 3 shows a larger fragment of high density alumina ceramic, taken with about 15 μm resolution. This image shows cracks, porosity and regions of lower absorption parameter which probably indicate large particles of a second phase.

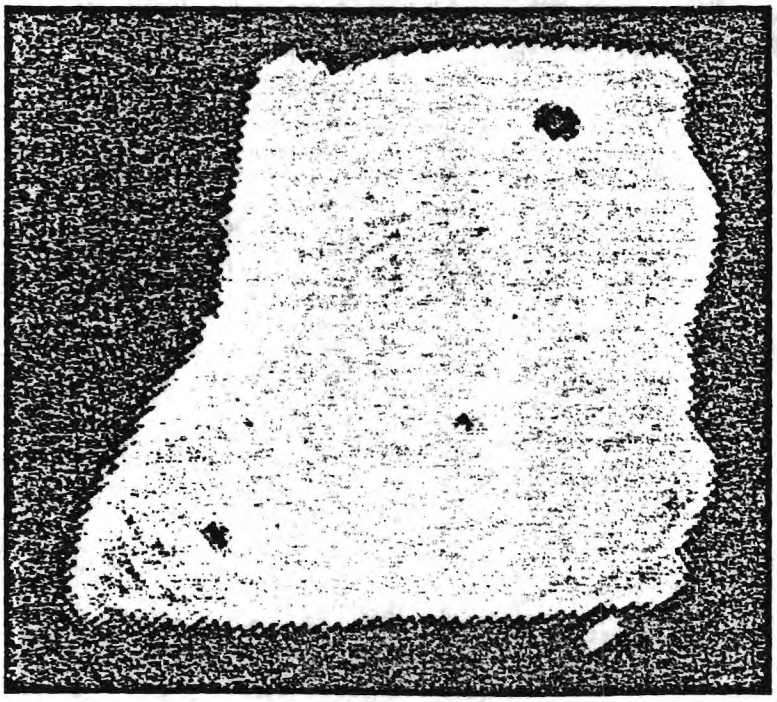

Figure 2. Reconstructed image of section of human femur bone, taken at 1 angstrom with a 4 μm collimator and a 5 μm stepsize.

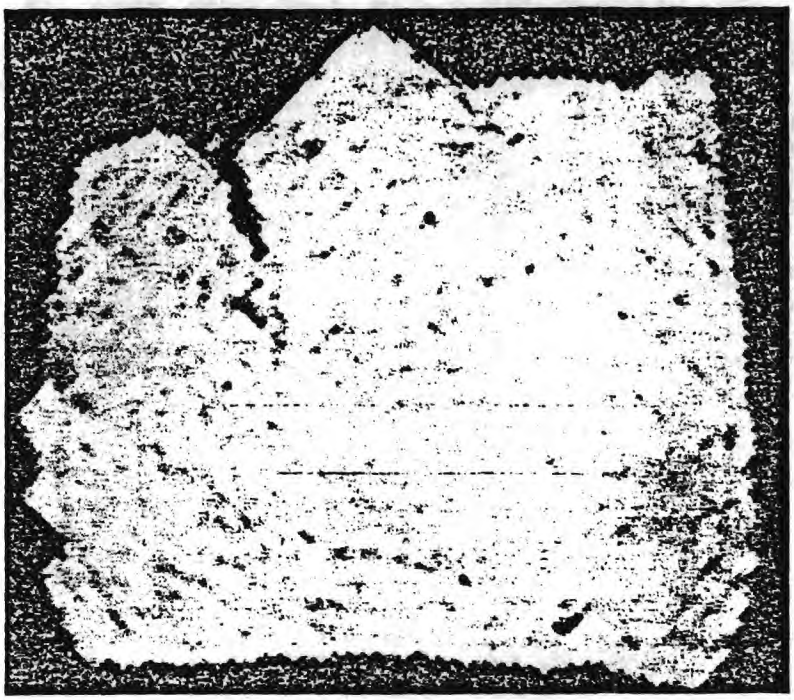

Figure 3. Reconstructed section of a fragment of high density alumina, taken with 0.3 angstrom radiation, a 30 μm aperture and a 15 μm stepsize

The choice of radiation wavelength is quite important. For best signal-to-noise in the reconstructed image it is necessary to have very approximately 50% absorption at the thickest part of the specimen. For precise reconstructions of absorption parameter rather than a qualitative density figure, it is necessary to have a fairly restricted range of wavelength since the absorption parameter varies with the cube of the wavelength. In practice a variation of a few percent in the wavelength is not detrimental and increases the available power. With synchrotron radiation sources, tuned monochromators are therefore highly convenient, but these must either be of the order-sorting broad band variety or the detector used must be capable of discriminating between λ and $\lambda/2$ for other harmonic wavelengths that may be present. For the wiggler line experiment, the wavelength of 0.35 angstroms was chosen to be just below the wavelength of the iodine absorption edge; this meant that the sodium iodide crystal in the detector was operating at high efficiency. It is seen that for versatile non-destructive investigation of materials of different sizes and average densities, considerable flexibility is required in the experimental arrangements and some thought must be given to the precise conditions for each measurement.

The data collection times for the above tomographs were approximately 4 hours, with the detector run close to saturation (i.e., the x-ray intensity was not a limiting factor). Approximately a quarter of this time was taken in simply moving the stepping motors to their new positions, when summed over the whole run. There are tremendous advantages to be gained from some form of parallel detection, which might be two-dimensional as in a charge coupled device or television camera, with sufficient integration to provide a high dynamic range, or even in the adoption of a few parallel channels provided that the spatial resolution of each channel is sufficient. It is quite easy to see developments in detector technology that would permit the data collection time to be reduced to minutes or even seconds with synchrotron radiation. The algorithms used for the reconstruction of the images are so far the conventional Fourier transform-based algorithms. It is quite possible that the effects of noise, which are quite evident in the images, could be better minimised by the use of algorithms based upon the maximum likelihood approach (Lange and Carson[8]). We are currently investigating the application of these methods.

In conclusion, computerised axial tomography with synchrotron radiation has demonstrated applicability to microstructural analysis at the micron level, in a completely non-destructive manner. We believe that this will have significant applications in the fields of biological materials, polymer and other composite materials, the study of processes such as sintering, and the study of phase mixtures in both geological and metallurgical specimens.

Acknowledgments

We acknowledge the provision of synchrotron radiation facilities by The Science and Engineering Research Council of the United Kingdom, and the assistance and co-operation of

staff of Daresbury Laboratory, in particular Dr. G.F. Clark and Dr. E. Pantos.

References

1. Hounsfield, G.N. British Journal of Radiology, 46, 1016 (1973).
2. Reimers, P., Gilboy, W.B., and Goebbels, J. NDT International, 17, 197 (1984).
3. Elliott, J.C., and Dover S.D. Metab. Bone Dis. and Rel. Res., 5, 219 (1984).
4. Elliott, J.C., and Dover S.D. J.Microscop. (in press).
5. Bowen, D.K.,and Davies S.T. Nucl. Instr. and Methods, 208, 725, (1983).
6. Elliott, J.C., Bowen D.K., and Dover S.D. Biological Trace Element Research (1986) (in press).
7. Lange K. and Carsons R. J.Computer Assisted Tomography, 8, 306 (1984).

NATIONAL SCIENCE FOUNDATION
Washington, D.C. 20550

FINAL PROJECT REPORT
NSF FORM 98A

PLEASE READ INSTRUCTIONS ON REVERSE BEFORE COMPLETING

PART I—PROJECT IDENTIFICATION INFORMATION

1. Institution and Address	2. NSF Program	3. NSF Award Number
Georgia Tech Research Corporation Georgia Institute of Technology Atlanta, Georgia 30332-0245	INT	INT-8513629
	4. Award Period From 3/1/86 To 12/31/88	5. Cumulative Award Amount $9,350

6. Project Title
Synchrotron Radiation Studies of the Spatial Distribution of Impurities in Materials

PART II—SUMMARY OF COMPLETED PROJECT *(FOR PUBLIC USE)*

Novel synchrotron radiation techniques were used to study the spatial distribution of impurities in materials. A number of techniques were proposed for investigation, and efforts in the project focused on topographic EXAFS and microtomography. Topographic EXAFS refers to contrast observed on x-ray diffraction images (e.g. topographs) due to the fine structure of the x-ray absorption edge. Microtomography is a very high resolution variant of the familiar medical CAT scanner. Experimental results are reported for crystals of gallium arsenide and hematite and for silicon carbide/silicon nitride and silicon carbide/aluminum composites. The technological and scientific impact of these experiments are also reported.

PART III—TECHNICAL INFORMATION *(FOR PROGRAM MANAGEMENT USES)*

1. ITEM *(Check appropriate blocks)*	NONE	ATTACHED	PREVIOUSLY FURNISHED	TO BE FURNISHED SEPARATELY TO PROGRAM	
				Check (✓)	Approx. Date
a. Abstracts of Theses	X				
b. Publication Citations		X			
c. Data on Scientific Collaborators		X			
d. Information on Inventions	X				
e. Technical Description of Project and Results		X			
f. Other *(specify)* i)presentations at national/ international meetings. ii)proposals resulting from program's accomplishment		X X			

2. Principal Investigator/Project Director Name *(Typed)*	3. Principal Investigator/Project Director Signature	4. Date
Stuart R. Stock		3/12/89

NSF Form 98A (1-87) Supersedes All Previous Editions

Form Approved OMB No. 3145-0058

PART IV - SUMMARY DATA ON PROJECT PERSONNEL

NSF Division INT-8513629

The data requested below will be used to develop a statistical profile on the personnel supported through NSF grants. The information on this part is solicited under the authority of the National Science Foundation Act of 1950, as amended. All information provided will be treated as confidential and will be safeguarded in accordance with the provisions of the Privacy Act of 1974. NSF requires that a single copy of this part be submitted with each Final Project Report (NSF Form 98A); however, submission of the requested information is not mandatory and is not a precondition of future awards. If you do not wish to submit this information, please check this box ☐

Please enter the numbers of individuals supported under this NSF grant.
Do not enter information for individuals working less than 40 hours in any calendar year.

*U.S. Citizens/ Permanent Visa	PI's/PD's		Post-doctorals		Graduate Students		Under-graduates		Precollege Teachers		Others	
	Male	Fem.	Male	Fem.	Male	Fem.	Male	Fem.	Male	Fem.	Male	Fem.
American Indian or Alaskan Native	0	0	0	0	0	0	0	0	0	0	0	0
Asian or Pacific Islander	0	0	0	0	0	0	0	0	0	0	0	0
Black, Not of Hispanic Origin	0	0	0	0	0	0	0	0	0	0	0	0
Hispanic	0	0	0	0	0	0	0	0	0	0	0	0
White, Not of Hispanic Origin	0	0	0	0	0	0	0	0	0	0	0	0
Total U.S. Citizens	0	0	0	0	0	0	0	0	0	0	0	0
Non U.S. Citizens	0	0	0	0	0	0	0	0	0	0	0	0
Total U.S. & Non-U.S. ..	0	0	0	0	0	0	0	0	0	0	0	0
Number of individuals who have a handicap that limits a major life activity.	0	0	0	0	0	0	0	0	0	0	0	0

*Use the category that best describes person's ethnic/racial status. (If more than one category applies, use the one category that most closely reflects the person's recognition in the community.)

AMERICAN INDIAN OR ALASKAN NATIVE: A person having origins in any of the original peoples of North America, and who maintains cultural identification through tribal affiliation or community recognition.

ASIAN OR PACIFIC ISLANDER: A person having origins in any of the original peoples of the Far East, Southeast Asia, the Indian subcontinent, or the Pacific Islands. This area includes, for example, China, India, Japan, Korea, the Philippine Islands and Samoa.

BLACK, NOT OF HISPANIC ORIGIN: A person having origins in any of the black racial groups of Africa.

HISPANIC: A person of Mexican, Puerto Rican, Cuban, Central or South American or other Spanish culture or origin, regardless of race.

WHITE, NOT OF HISPANIC ORIGIN: A person having origins in any of the original peoples of Europe, North Africa or the Middle East.

THIS PART WILL BE PHYSICALLY SEPARATED FROM THE FINAL PROJECT REPORT AND USED AS A COMPUTER SOURCE DOCUMENT. DO NOT DUPLICATE IT ON THE REVERSE OF ANY OTHER PART OF THE FINAL REPORT.

TABLE OF CONTENTS **Page**

PART III

b. Publication Citations

1. "X-ray Microtomography with Synchrotron Radiation," D. K. Bowen, J. C. Elliott, S. R. Stock and S. D. Dover, in X-ray Imaging II, SPIE Vol. 691, (1986) 94.

2. "Microtomography of Silicon Nitride/Silicon Carbide Composites," S. R. Stock, A. Guvenilir, T. L. Starr, J. C. Elliott, P. Anderson, S. D. Dover and D. K. Bowen, accepted for Advanced Techniques for Characterization of Ceramics (Am. Cer. Soc./MRS, 1989).

Anticipated Publications, Journal (if known) and Submission Dates

1. "Detectability of Cracks in Continuous-Fiber, Metal Matrix Composites Using Microtomography," T. M. Breunig, S. R. Stock, J. C. Elliott, A. Guvenilir, S. D. Antolovich, P. Anderson, S. D. Dover and D. K. Bowen, est. June 1989.

2. "Processing Induced Porosity and Density Variation in Silicon Carbide/Silicon Nitride Ceramic Matrix Composites," A. Guvenilir, S. R. Stock, J. C. Elliott, T. L. Starr, P. Anderson, S. D. Dover and D. K. Bowen, Phil Mag A, J. Am. Cer. Soc. or J. Mat. Res., est. June 1989.

c. Data on Scientific Collaborators

The various individuals who participated in different parts of the cooperative science project are listed below:

Georgia Institute of Technology

Mr. A. Guvenilir (Materials Engineering)
Mr. T. M. Breunig (Materials Engineering)
Dr. T. L. Starr (GTRI)
Dr. S. D. Antolovich (Materials Engineering)

London Hospital Medical College (LHMC)

Drs. J. C. Elliott and P. Anderson
Department of Child Dental Health
London Hospital Medical College
Turner Street
London E1 2AD, U.K.

Kings College, University of London

Dr. S. D. Dover
Kings College
University of London
London, U.K.

University of Warwick

Dr. D. K. Bowen
Department of Engineering
University of Warwick
Coventry CV4 7AL, U.K.

Stanford Synchrton Radiation Laboratory

Dr. Z. U. Rek
SSRL
P. O. Box 4349, Bin 69
Stanford, CA 94309-0210

e. Technical Description of Project and Results

1. Introduction

The initial goal of this cooperative science project was to develop and to apply synchrotron x-ray diffraction imaging, microbeam x-ray fluorescence mapping and differential absorption microradiography to the study of the spatial distribution of impurities in materials. The collaborative experiments were to be conducted at Daresbury Laboratory with Dr. D. K. Bowen's group (Department of Engineering, University of Warwick, U.K.). Five types of specimens were identified for study: porous-sintered samples (microradiography), single crystals with composition gradients (diffraction imaging), samples with grain boundary segregation (microbeam x-ray fluorescence) coal (microradiography) and porous materials for medical implants (microradiography).

The unavailability of the Daresbury Synchrotron Radiation Source (SRS) during much of the period in which the experiments were to be conducted.

Installation of the high brightness lattice closed SRS to experimenters from October 1986-June 1987. It has also been exceedingly difficult to obtain time on the topography wiggler line; use of this line is necessary for most of the planned experiments. This has been due, apparently, to a shift in scheduling priorities: beam time has been approved for our experiments but little has been allocated for this class of experiments. Related to the lack of beam time are delays in our collaborator's microbeam fluorescence project; optics development for focusing to 10 μm beam diameter has been protracted.

A second change in the actual research performed was to substitute microtomography for microradiography. Microtomography has developed very rapidly over the last five years, and its advantages over conventional projection radiography are considerable. This, coupled with the fact that our British collaborators are leaders in the field of microtomography, dictated the shift from microradiography to microtomography. Due to the lack of beam time at Daresbury much of the collaborative microtomography has been done using laboratory radiation.

Two of the three techniques have been examined (x-ray absorption and topographic EXAFS methods) and two of the five sample types were studied in detail (porous composite samples and single crystal specimens). Studies of precipitates in coal were abandoned when we learned that other investigators were devoting large efforts [1,2]. The microfluorescence and biomaterial experiments have not yet been pursued (the former, noted above, because of instrumental problems). The following section reviews the techniques, the results of which are summarized and discussed in the third section of the report.

The fourth section describes the technological and scientific impact of the collaborative research.

2. Background

Microtomography

In computed tomography and high resolution variants termed microtomography, the spatial variation of x-ray absorption in a thin slice or cross-section of the sample is recorded for various projection directions or views, the number of which depend on the ultimate resolution desired [1]. The different views are combined via a reconstruction algorithm, and the two-dimensional map of x-ray absorption across the slice is obtained [3,4]. The three-dimensional distribution of absorption in the sample is recovered by stacking successive slices. This approach is much superior to microradiography where features of interest can be obscured if the sample is too thick or if there are too many overlapping features. Cracks and their precursors are much more readily detected with computed tomography because geometric invisibility is no longer possible (geometric invisibility occurs when a crack is viewed from directions other than its plane: virtually no contrast is produced because the path length though the material is unchanged).

Spatial resolution has always been a limitation of tomography apparatus. Medical units have resolution approaching 0.5 mm in most cases, although a specialized industrial unit with 50 μm resolution has been described for samples with dimensions on the order of inches [5,6]. Systems using ribbon-like x-ray beams (from rotating anode sources) and multiple detector arrays are limited to

spatial resolution no better than 25 μm because of the intrinsic dimness of conventional x-ray sources.

Elliott and Dover [7] used the translate-rotate scheme (the specimen is translated across a very narrow diameter beam to obtain each absorption profile, and then the sample is rotated for the next view), a microfocus x-ray generator and a 15 μm diameter collimator to obtain very high resolution microtomographs of human femoral bone. Their apparatus is shown schematically in Fig. 1. Counting time per slice was about 19 h for a 0.8 x 0.8 mm^2 sample (128 points, each counted for 10 s, per projection and 54 projections at 3 1/3° intervals per slice), and undersampling (~130 projections should have been recorded) blurred the image.

Data acquisition rates can be improved with the LHMC scanner if synchrotron radiation is used. Synchrotron radiation is produced when electrons traveling at relativistic velocities are deflected by the bending magnets, wigglers or undulators of a storage ring. The brightness of synchrotron white radiation is at least two orders of magnitude higher than that of characteristic peaks from the most powerful laboratory sources [8]. The broad spectrum of synchrotron radiation allows selection via monochromators of the most appropriate wavelengths for a given specimen; one is not limited to wavelengths of characteristic lines. Spatially-broad and well-collimated beams are natural property of synchrotron radiation and provide a considerable advantage over conventional x-ray sources. Bowen, Elliott, Stock and Dover [9], as part of this cooperative science project, used the LHMC apparatus and synchrotron radiation to study human femur bone and sintered alumina with 4 and 10 μm diameter collimators, respectively. Counting times were 1 s/position (128 positions/profile) for the 2 mm square alumina

specimen, and 64 views of the sample were recorded in about 4 h.

The LLNL and EXXON groups have chosen to use parallel data collection [1,2]. The LLNL group uses a fluorescent screen coupled through a lens to a CCD (charge coupled device) array and have obtained spatial resolution of about 5 μm at the Stanford Synchrotron Radiation Laboratory (SSRL) and at the German Electron Synchrotron Source (DESY) [1]. A schematic of their apparatus is shown in Fig. 2. Many absorption profiles are recorded simultaneously so that the data collection rate is orders of magnitude faster.

Topographic EXAFS

X-ray diffraction topography uses a nearly parallel beam of x-rays to image the diffraction and orientation contrast from crystals or from large grained polycrystalline samples. The contrast mechanisms are similar in most respects to those in TEM. In white beam topography a pattern of Laue spots is formed, each of which is an individual topograph produced by diffraction of a specific wavelength and its harmonics. Dispersion from the finite synchrotron source size or variations in the crystal's orientation (due to bending) leads to a small range of wavelengths being diffraction from different positions of the sample. If the specimen is aligned to diffract a range of wavelength encompassing that of the absorption edge of an element of the sample, large contrast differences can be observed across the specimen [10]. The technique, termed topographic EXAFS, appears to be promising for simultaneous assessment of crystalline and chemical defects in crystals. It may be able to serve as a survey tool to identify specific regions of the crystal for more detailed examination with techniques such as microbeam EXAFS.

3. Description of Samples Examined and Results Obtained

Materials

The materials examined include a commerical alumina refractory, two fiber-matrix composites and two crystals containing composition gradients. The composites studied by microtomography were an aligned-fiber metal matrix composite, SiC/Al, and a chopped-fiber ceramic matrix composite, SiC/Si_3N_4. The crystals examined for topographic EXAFS effects were GaAs, which contained a variation in stoichiometry from seed to tail, and hematite, which is suspected of having a Fe valence change near twin boundaries. Thus, a wide range of sample types were evaluated in this program.

The initial microtomography experiment was on a porous alumina refractory. This sample had pores up to two millimeters in diameter and is typical of commercially available material. The majority of microtomography, however, was on advanced composites where the information obtained would have greater scientific and technological impact.

The addition of SiC or other dispersoids (particles, whiskers or fibers) to silicon nitride matrices offers a potential for considerable improvement of fracture toughness and strength [11]. Apparently, the strong ceramic fibers can prevent catastrophic brittle failure by providing extra energy dissipation during crack advance [12]. The silicon nitride matrix/silicon carbide fiber system has received considerable attention [12-16] particularly since commercial, continuous-polymer derived SiC fibers such as Nicalon provide good chemical compatibility and degradation resistance superior to carbon fibers in high temperature oxidizing environments. Complete densification of sintered or chemical vapor infiltrated (CVI) specimens is frequently impossible, however, due to the formation of stable pores in the interior of grains or to the

enclosure of pores by growth of the matrix on surrounding fibers. The resulting lower density and large number of internal stress concentrators leads to poor mechanical properties. If the porosity cannot be eliminated during processing, most of the anticipated fracture toughness will be lost.

Continuous fiber reinforced SiC/Al MMC are designed for high temperature structural applications in the aerospace industry. Composites similar to these (but as yet undefined) are envisioned for application in the National Aerospace Plane (NASP), the Advanced Tactical Fighter (ATP), manned space stations, etc. A major effect on the mechanical properties of MMC's is the damage induced by thermal cycling. As the structure undergoes a thermal cycle, the coefficient of thermal expansion mismatch between fiber and matrix initiates fatigue damage and debonding at the fiber/matrix interface. The damage is very difficult to detect experimentally because of crack closure when the externally applied loads are removed. The current methods for assessing the damage state are based upon stiffness loss [17-19]. They do not, however, provide an adequate indication of the location and quantity of damage present. Knowledge of the crack initiation and propagation stages, a measure of the total quantity of damage present and a descriptive model for damage evolution are required for prediction of the remaining life of a structure.

The advanced composites which were studied with microtomography were random fiber SiC/Si_3N_4 CMC and continuous fiber SiC/Aℓ MMC. The SiC fibers were 15 and 142 μm in diameter for the CMC and MMC materials, respectively. The CMC was studied to establish sensitivity of microtomography to processing defects, and the MMC was studied to define damage/crack detectability limits for different levels of spatial resolution.

The crystals examined for topographic EXAFS effects were GaAs and Fe_2O_3. Variations in valence of the Fe atoms were expected across the crystal as were variations in stoichiometry in the GaAs crystal. The GaAs crystal was a longitudinal slab from a melt-grown crystal. Variations in stoichiometry produce differences in electrical properties, and it is important to minimize these differences in wafers taken from different portions of a boule. Measuring these chemical differences and comparing them to changes in electrical properties is the first step in evaluating the magnitude of needed improvements in composition control during crystal growth. Anomalous contrast was observed near twin boundaries in topographs of the Fe_2O_3 crystal, and one possible source was localized changes in valence of Fe and a corresponding change in the atomic scattering factor [20]. Our experiments were to test this hypothesis.

Topographic EXAFS

These experiments were performed at the Stanford Synchrotron Radiation Laboratory (SSRL) because of the Daresbury shutdown and because of Dr. Bowen's sabbatical in the U.S. A particular reflection for each sample was chosen to minimize the harmonics contained in the topographic image (e.g. $\underline{h}$=220 for GaAs) and to enhance any topographic EXAFS contrast. The specimen was aligned normal to the beam and then rotated so that the reflection of interest was diffracted in transmission and at a wavelength near that of the absorption edge (Ga for GaAs and Fe for Fe_2O_3). Further alignment was accomplished by recording in situ transmission Laue patterns: with an incident white beam many diffraction spots are formed, each with a different wavelength.

We attempted to monitor the critical reflection using a Brimrose x-ray videocamera system, but the background was too high for the fine structure to

be resolved within the spot. We located the edges of both the GaAs and Fe_2O_3 crystals by exposing a large number of polaroids and observing whether the contrast changed after small rotations. Topographs were recorded at wavelengths on either side of the absorption edges using the minimum rotation steps of the SSRL topography camera. The change in contrast is so gradual that detailed numerical image analysis will be required before this experiment can evaluated. The image analysis will be conducted by the British group using Daresbury Laboratory facilities. The poor performance of the Brimrose videosystem (which, to be fair, may have been malfunctioning) serious hindered the progress of this portion of the program.

Microtomography

The synchrotron of microtomography alumina was conducted at the Daresbury Topographic Wiggler Station under the author's exploratory beam time grant "Synchrotron Computed Tomography Study of the Distribution of Pores in Sintered Alumina." The apparatus used is diagrammed in Fig. 1 and was designed and constructed by Dr. J. C. Elliott, London Hospital Medical College and Dr. D. K. Bowen, University of Warwick. Image reconstruction was done using software of Dr. S. D. Dover, King's College, London.*

The collimator diameter was 10 μm and the translation steps were 15 μm. The counting time was 0.75 seconds per position. Absorption was measured for x-rays with λ=0.37A by means of a post-specimen monochromator. After each profile was obtained, the specimen was rotated by 3.0 degrees, and the process

*For more information, please see the reprints [9] submitted with the annual report.

was repeated until the specimen had been viewed from 180 degrees. In the limited beam time, five slices of the 2x2x10 mm^3 alumina samples were obtained. Four of the five scans were made with a 10 μm diameter collimator and are from adjacent volumes of materials (each slice is separated by 20 μm). The other scan was recorded using a 30 μm diameter collimator. A number of pores and a crack or very large cavity intersecting the surface were seen [9].

Laboratory microfocus radiation was used to study porosity as a function of processing conditions in SiC/Si_3N_4. We recorded a large number of adjacent slices with a 10 μm diameter collimator, and differences in porosity were clearly evident. The sample shown in Fig. 3 and 4 was produced by reaction bonding, was approximately 1 mm^2 in cross-sectional area and contained considerable porosity. Each pixel in the reconstructed images is about 20 and 10 μm on a side in Fig. 3 and 4, respectively. The higher resolution in Fig. 4 is due to the larger number of views recorded for these slices. The lighter areas represent regions of low x-ray absorption, and the slices are reproduced with 256 gray levels. Adjacent slices (numbered) are separated by 20 μm, large trapped pores and highly densified volumes are clearly visible, but individual 15 μm fibers are not resolved in these tomographs. Tomographs were also recorded from a second Si_3N_4/SiC composite which had been processed to eliminate the porosity. As expected, these tomographs revealed little porosity with dimensions greater than 10 μm. A preliminary report on these results should appear shortly [21]; preprints are enclosed with this report.

One key element in the analysis is the resolution of individual fibers whose x-ray absorption is quite similar to the matrix and whose 15 μm diameter is only slightly larger than the ~10 μm pixel size. The random orientation of

the fibers necessitates three-dimensional presentation of the adjacent slices; limited ranges of absorption will be rendered so that the resulting skeletal image will emphasize connected porosity or fibers. The data also allows determination of the average density of the sample; when this part of the analysis is complete, this density can be compared with that determined by macroscopic techniques. The distribution of pore sizes is also currently under investigation. A paper for submission to an archival journal (such as Philosophical Magazine A, Journal of Materials Research or Journal of the American Ceramics Society) will follow the completion of the analysis.

Damage in a continuous fiber SiC/Al MMC has also been studied with laboratory microfocus radiation apparatus; the sample was split parallel to and between the unidirectional fibers by a wedge [22]. The resulting crack stayed between plies of fibers for the most part, although SEM micrographs of the side of the sample revealed some micro-cracking and fiber breakage. The wedge was left embedded in the sample so that a gradient of crack openings and their visibility could be studied with microtomography (Fig. 5). Resolution in the slices was quite poor due to the fact that the wedge required a large sample to collimator separation; the divergence of the beam irradiated a much larger volume than was ideal. The limit of crack detectability cannot, therefore, be determined from this data. We can, however, determine the minimum crack opening displacement which produced significant contrast for this particular pixel size. The volume fraction of crack within the pixel can be estimated from the observed contrast and can be correlated with an extrapolation of crack openings measured at different distances from the wedge. When complete, this work will also be published in the open literature.

4. Scientific and Technological Impact

The power of microtomography for processing defect characterization and for damage determination in MMC and CMC has been demonstrated. This study has shown that microtomography can lead to improved understanding of damage and of processing-related defects in composites. This is a prerequisite for improved life-prediction and process modeling, for wider use of composites and for extensive economic impact of this strategy for obtaining enhanced properties. Better understanding of damage mechanisms and their relationship to processing defects will be the first step to a new generation of high performance composites. The nondestructive nature of tomographic "sectioning" of the sample allows the same specimen to be studied multiple times during processing or deformation tests and allows the clearest identification of the mechanisms controlling macroscopic properties. Sample-to-sample variability, which often plagues composite studies, can now be eliminated.

Higher resolution must be obtained, and better means for presenting the three-dimensional data must be devised. Correlation of tomographic images with well-understood and accepted techniques such as fractography are necessary for the confident interpretation of results. Development of this type of database on relatively complex materials such as composites will lay the groundwork for widespread, routine NDE of composites and of monolithic materials with these techniques. Achievement of 1 μm resolution over millimeter-wide dimensions will fill the gap between electron microscopy and statistical sampling techniques such as small angle scattering on the one hand and macroscopic measuring techniques on the other. The previously inaccessible size range is where microscopic mechanisms link with macroscopic behavior (and associated continuum models), and,

as such, its study is critical for physically based modeling.

Progress in the fundamental understanding of damage accumulation in CMC, PMC and MMC appears very likely if microtomography is developed further. Advances in the technique's sensitivity and spatial resolution must, therefore, be an important goal. Increasing the volume of material which can be studied with microtomography is critical if it is to be used with specimens for which fracture mechanics calculations are valid (e.g. 1 cm^2 cross-sections instead of the 2 mm^2 which are presently feasible). Resolution of 1 μm and contrast better than 4% are goals which can be met in the next few years. The examination of larger diameter samples will also be possible, and it is not too optimistic to envision microtomography studies of samples with 5 mm or greater diameters. Another issue central to NDE of structural composites and to understanding basic failure mechanisms is the role of the loading state in the detectability of cracks. It is essential to know whether complex loading stages will be needed for routine NDE imaging. If damage is hidden by the removal of loads (if cracks or fiber-breaks close when the imposed strain is released), the amount of "invisible" damage or its fractions of the total damage should be established. Finally, the relationship of damage accumulation to processing flaws or to fiber arrangement must be determined.

Effort should concentrate, therefore, on the fundamental aspects of damage initiation and accumulation, on the link between microscopic features and macroscopic mechanical behavior of composites and on microstructure-based modeling of phenomena such as stiffness loss. The understanding developed will be a key to improved composite design and processing, and industrial interactions will be essential in assuring improvements in the next generation of composite

materials. Making use of and refining instrumentation advances made elsewhere, promises exceptional scientific and technological advances for a very modest level of effort. Interpretation of data will be much clearer because the sample samples can be examined many times during the course of the deformation test. This approach of microtomographic damage characterization will, therefore, provide exciting, and perhaps unprecedented, advances in understanding damage initiation and accumulation.

References

1. J. H. Kinney, Q. C. Johnson, U. Bonse, M. D. Nichols, R. A. Saroyan, R. Nusshardt, R. Pahl and J. M. Brase, MRS Bul. **XIII**#1 (1988) 13.

2. B. P. Flannery, H. Deckman, W. Reberge and K. D'Amico, Science **237** (1987) 1439.

3. G. T. Herman, Image Reconstruction from Projections: The Fundamentals of Computerized Tomography, Academic Press (1980).

4. A. C. Kak and M. Slaney, Principles of Computerized Tomographic Imaging, IEEE Press (1988).

5. F. H. Seguin, P. Burstein, P. J. Bjorkholm, F. Homburger and R. A. Adams, Appl. Optics **24** (1985) 4117.

6. R. A. Armistead, Advanced Matls. and Processes/Metals Progress, March 1988, p. 42.

7. J. C. Elliott and S. D. Dover, J. Microscopy **138** (1985) 329.

8. U. Bonse, in: Characterization of Crystal Growth Defects by X-ray Methods (1980) 298.

9. D. K. Bowen, J. C. Elliott, S. R. Stock and S. D. Dover, in: X-ray Imaging II **SPIE 691** (1986) 94.

10. D. K. Bowen, S. R. Stock, S. T. Davies, E. Pantos, Haydn Chen and H. V. Birnbaum, Nature **309** (1984) 336.

11. S. T. Buljan, J. G. Galdoni and M. L. Huckabee, Ceramic Bul. **66** (1987) 347.

12. J. Homeny and W. L. Vaughn, MRS Bul. Oct. 1/Nov. 15 (1987) 66.

13. T. -I. Mah, M. G. Mendiratta, A. P. Katz and K. S. Madiyasni, Ceramic Bul. **66** (1987) 304.

14. R. Lundberg, L. Kahlman, R. Pompe, R. Carlsson and R. Warren, Ceramic Bul. **66** (1987) 304.

15. T. L. Starr, J. N. Harris and D. L. Mohr, in Ceramic Sci Proc. **8** (1987) 985.

16. T. L. Starr, in: Tenth International Conference on Chemical Vapor Deposition (1987) 1147.

17. W. Hwang and K. S. Han, J. Composite Matls. **20** #3, (1986) 125.

18. W. S. Johnson, NASA Tech. Mem 89116, March 1987.

19. J. Aboudi, Composites Science and Technology **28** (1987) 103.

20. D. K. Tanner, private communications (1985).

21. S. R. Stock, A. Guvenilir, T. L. Starr, J. C. Elliott, P. Anderson, S. D. Dover and D. K. Bowen in: Advanced Characterization Techniques for Ceramics (in press).

22. T. M. Breunig, S. R. Stock, A. Guvenilir, J. C. Elliott, P. Anderson, S. D. Dover, D. K. Bowen and S. D. Antolovich, unpublished data.

23. S. R. Stock, J. H. Kinney, T. M. Breunig, U. Bonse, S. D. Antolovich, Q. C. Johnson and M. C. Nichols, in: Synchrotron Radiation in Materials Research (in press).

f. Presentations at National and International Meetings

1. "Microtomography os Silicon Nitride/Silicon Carbide Composites," S. R. Stock, et al., TMS-AIME, 1988 Fall Meeting, Chicago, Illinois, September 29, 1988.

2. "Microtomography of Silicon Nitride/Silicon Carbide Composites," S. R. Stock, et al., Symposium on Advanced Characterization Techniques for Ceramics (Am. Cer. Soc./MRS), San Francisco, California, October 24, 1988.

3. "Application of Microtomography to the Study of Ceramic and Metal Matrix Composites, S. R. Stock, Symposium on Thermal and Mechanical Behavior of Ceramic and Metal Matrix Composites (ASTM), Atlanta, Georgia, November 8, 1988.

4. "Application of Microtomography to Composites," S. R. Stock, et al., Symposium V: Synchrotron Radiation in Materials Research (MRS), Boston, Massachusetts, November 30, 1989.

5. "Microtomography of Damage in SiC/Al Continuous Fiber Composites," T. M. Breunig, S. R. Stock, et al., TMS-AIME, 1989 Annual Meeting, Las Vegas, Nevada, February 28, 1989.

Proposals Resulting from Program Accomplishments

1. "US-UK Cooperative Research - Novel X-ray Methods for Characterization of the Spatial Distribution of Inhomogeneities in Materials," NSF INT-8814774, $15,067, 11/1/88-4/30/92.

2. "US-France Cooperative Research: Characterization of Damage in Composites by Microradiography, Computed Tomography and Microtomography." NSF Proposal INT-8815501, not funded.

3. "Computed Tomography Apparatus for Evaluation of Consolidation during Processing of Monolithic and Composite Ceramics," E. J. Grassmann Trust, $20,000, July 1988.

4. "A Study of the Relationship between Macroscopic Measures and Physical Processes Occurring during Crack Closure," ONR, $303,107, 3/89-2/91.

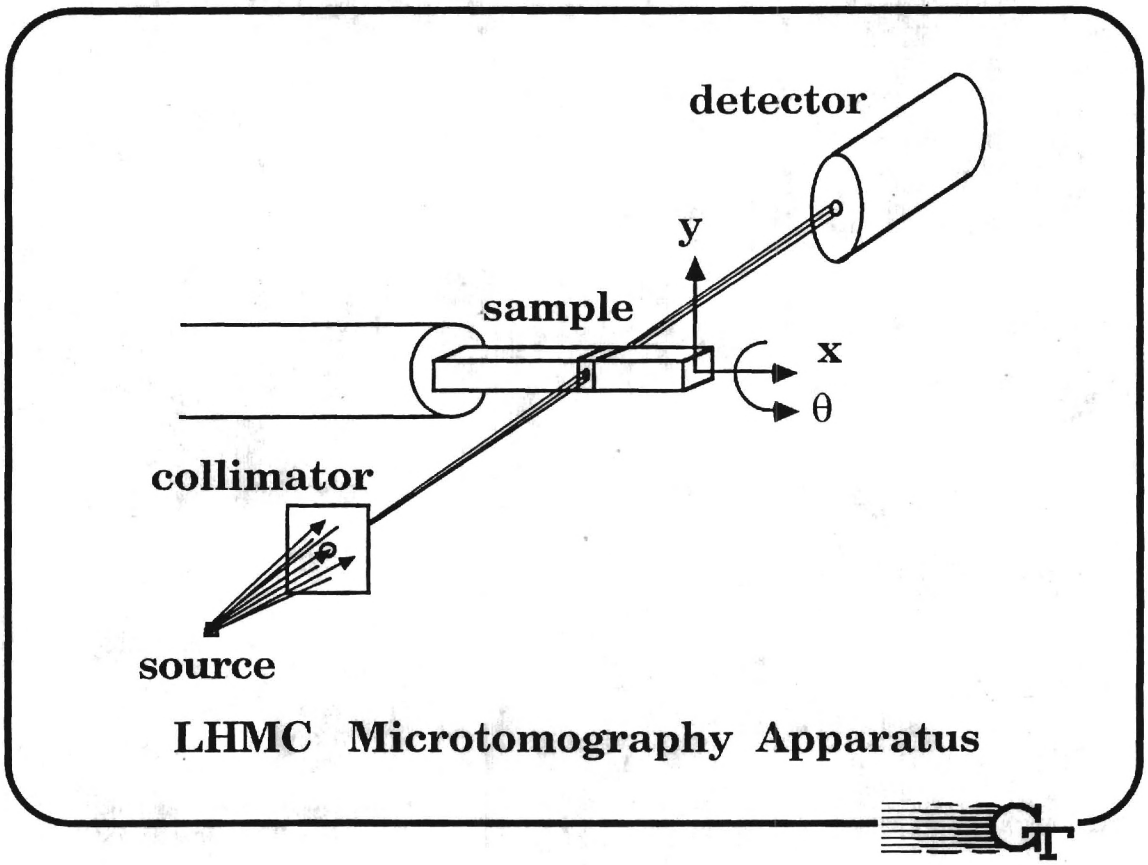

Figure 1. Schematic of the London Hospital Medical College pinhole microtomography apparatus.

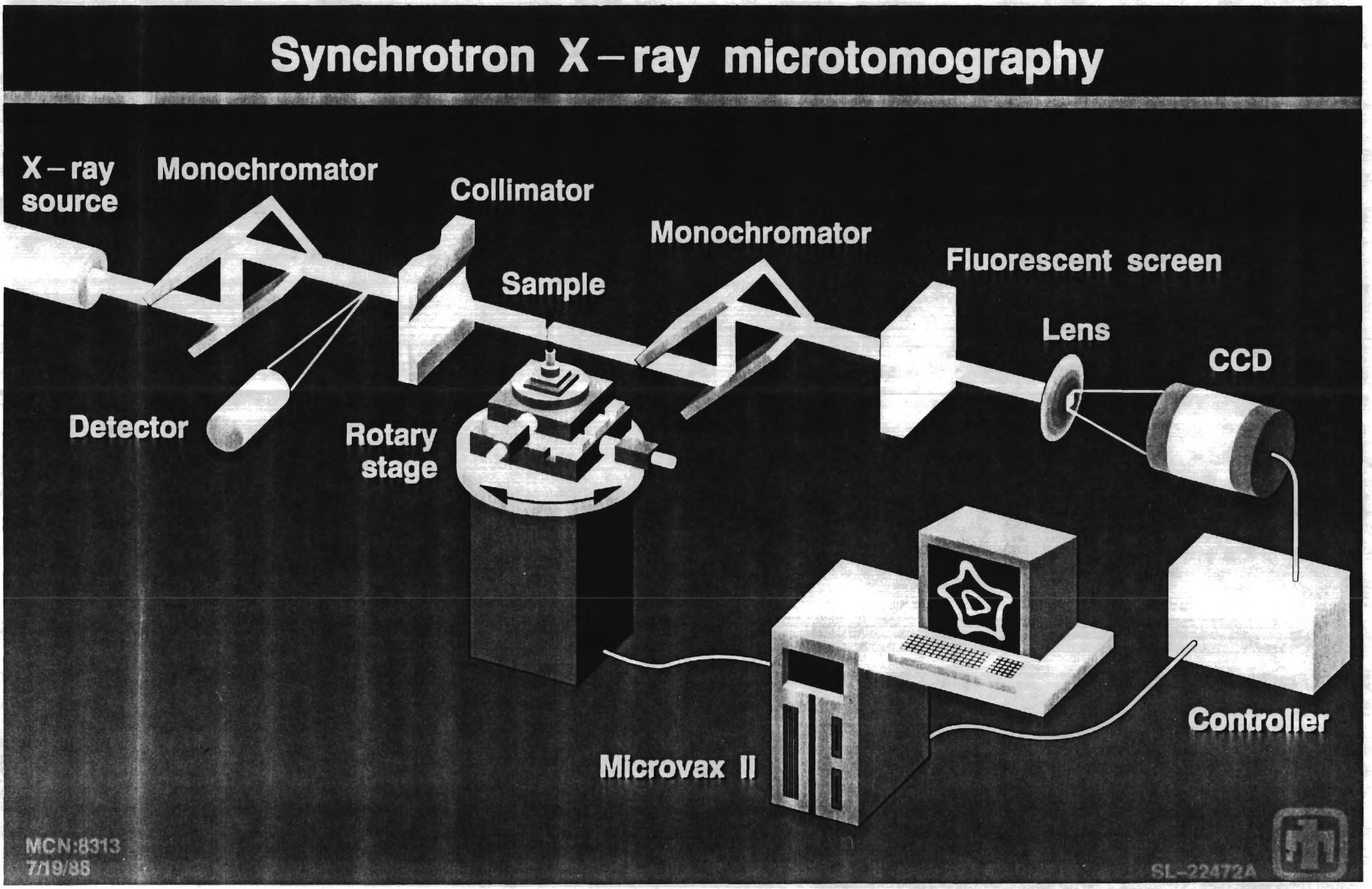

Figure 2. Schematic of the Lawrence Livermore National Laboratory CCD-based microtomography apparatus.

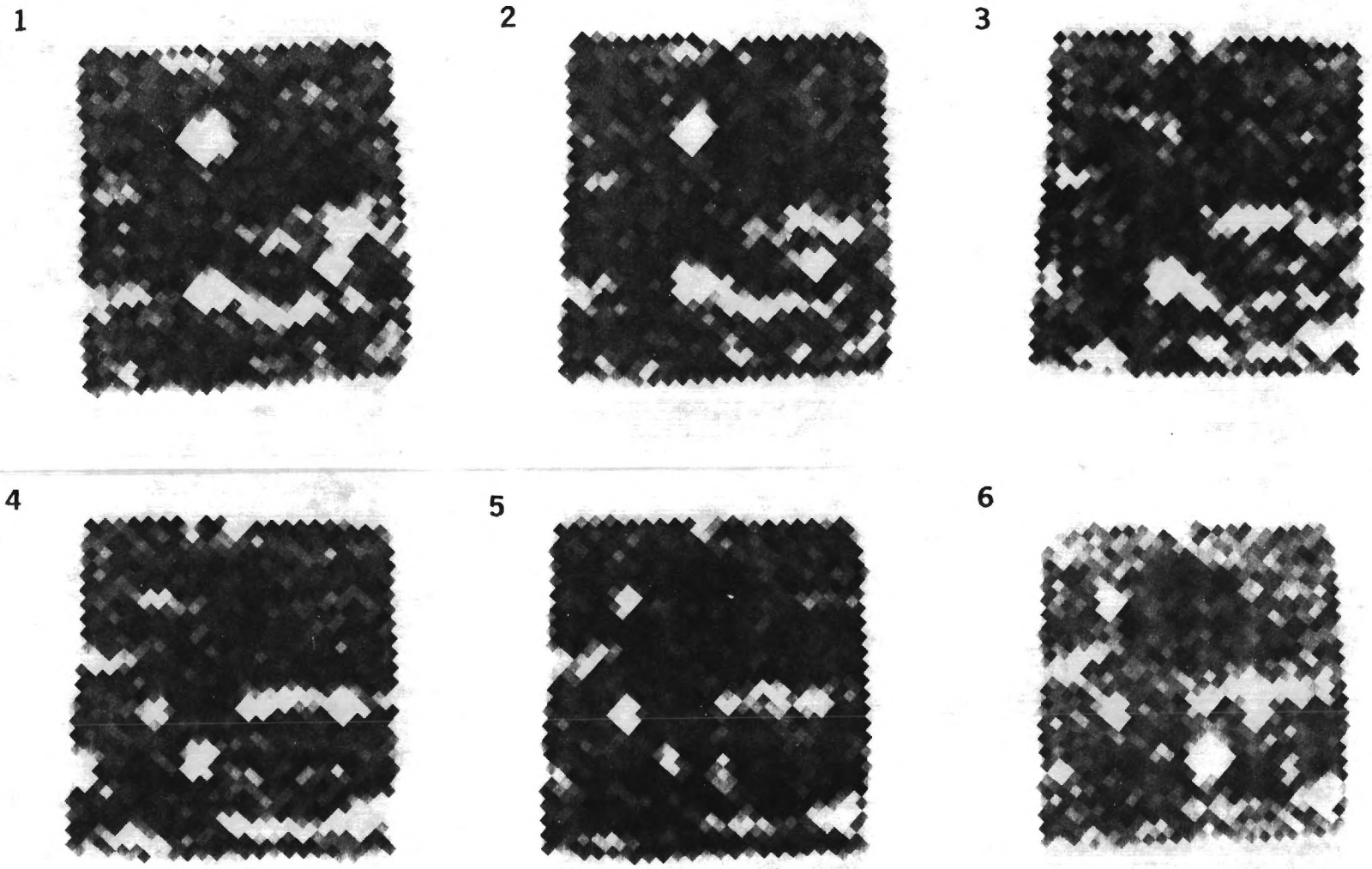

Figure 3. Silicon nitride/silicon carbide composite (1 mm^2 cross-section)
Sample N-1-4 (porous) Reconstructions SIL
10 um dia. collimator, 20 um between slices, 3 deg/ view
Darker pixels have higher x-ray absorption.

Figure 4.

Silicon nitride/silicon carbide composite (1 mm2 cross-section)
Sample N-1-4 (porous) Reconstructions SIL3
10 um dia. collimator, 10 um between slices, 1.5 deg/ view
Darker pixels have higher x-ray absorption.

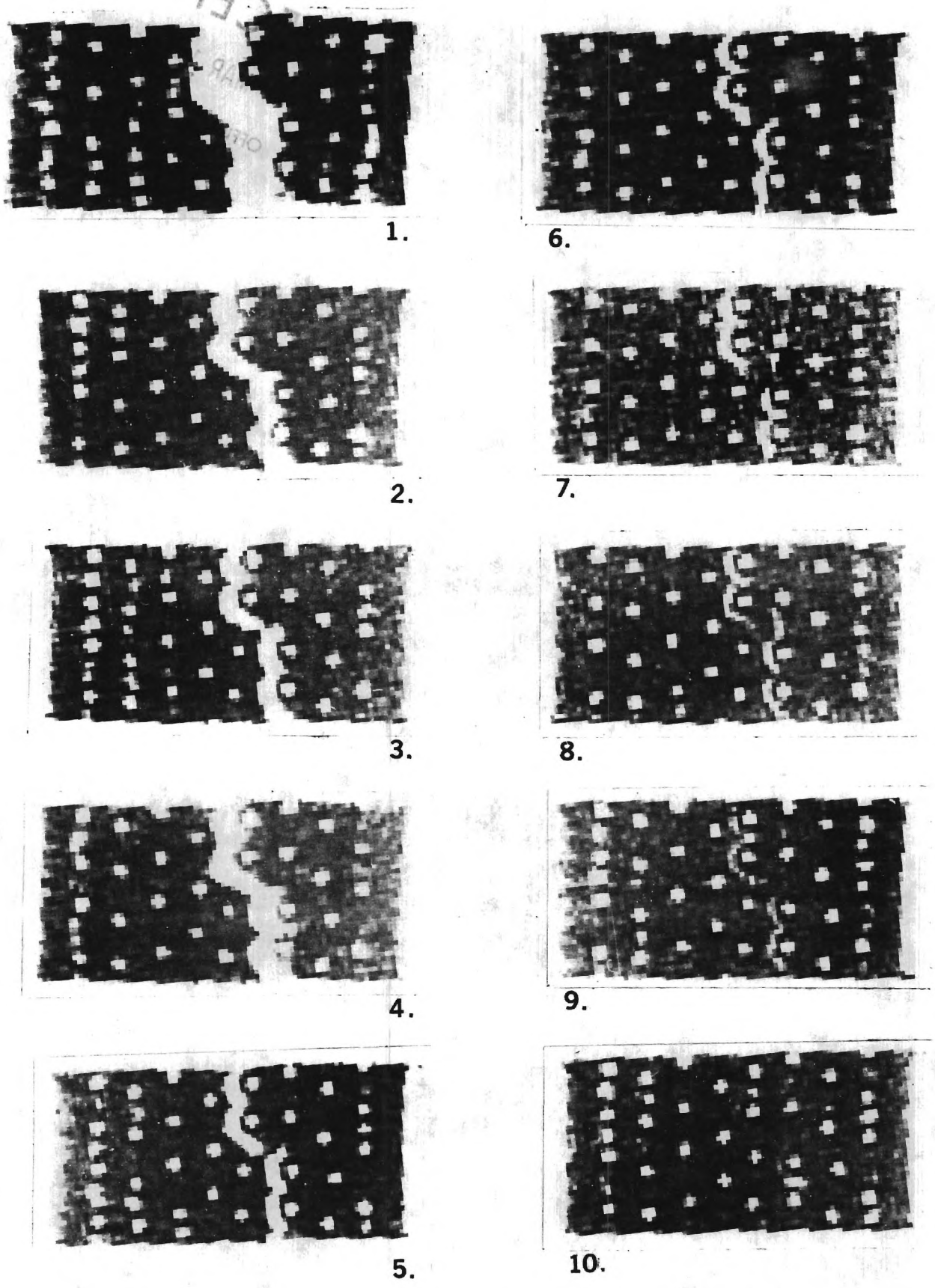

Figure 5. Slices perpendicular to a crack in a SiC/Al MMC, illustrating the variation in crack opening with distance from the wedge. The lower numbers are closer to the wedge.